GEORGIAN BIOMEDICAL NEWS

ISSN (Online): 2720-8796 ISSN (Print): 2720-7994 VOLUME 1. ISSUE 2. APRIL-JUNE 2023

# Infrared Visualization of Prostate Cancer Tissues with Various Gleason Scores

Sopio Abazadze[1], Alexandre Khuskivadze[1], Besarion Partsvania[2], Tamaz Sulaberidze[2], Davit Kochiashvili[1], Omar Khardzeishvili[3]

DOI: 10.52340/GBMN.2023.01.01.26

ABSTRACT

BACKGROUND: Prostate cancer is the second most significant cause of male mortality, beneath lung cancer. Prostate-specific antigen (PSA) and digital rectal examination (DRE) play the most critical roles in identifying prostate cancer, and their use has risen with the incidence of prostate cancer worldwide. Cancer-specific mortality has been reduced as a result of these tests. On the other hand, the PSA and DRE led to overdiagnosis, overtreatment, and inappropriate prostate cancer testing. This situation led to modifications in prostate cancer recommendations, most notably by the US Preventive Services Task Force (USPSTF) in 2012.

OBJECTIVES: This study evaluated the infrared transmittance of transrectal prostate biopsy tissue to see a possible difference between the total and biopsy tissue. We also saw variations based on the total of Gleason's scores. To fulfill the stated aim, in the following tasks, (i) we investigated the relationship between prostate tissue resolution and radiation wavelength in the spectrum's infrared area, and (ii) elaborated software that allowed the received images to be processed in an infrared environment and detect prostate cancer tissue with a 95% confidence interval.

METHODS: 174 formalin-fixed and paraffin-embedded (FFPE) cases (prostate biopsies) were included in the study. There were five groups based on Gleason score (GS 6 [3+3], GS 7 [3+4], GS 7 [4+3], GS 8 [3+5], [4+4], [5+3], and GS 9 [4+5] and 10 [5+5] were combined). After the infrared exposition of each FFPE biopsy sample, our algorithm generated the image. Furthermore, the findings were matched to histomorphology reports. We employed the software's integrated statistical analysis and students' t-distribution.

RESULTS: The experiment revealed that when the Gleason score sum was 6 (3+3) and 7 (3+4) or 7 (4+3), image intensities in the infrared environment were almost indistinguishable from each other with 95% confidence, which cannot be said for prostate tissue with a higher Gleason score sum (8 (4+4; 3+5); (5+3) and 9-10). However, these changes were not evident in the first three groups since the experiment was conducted on biopsy material with a tissue thickness of 1 mm.

CONCLUSIONS: Infrared radiation can identify prostate cancer in prostate biopsy tissues. However, further investigations are needed to validate the modality's effectiveness for prostate cancer diagnosis.

KEYWORDS: Infrared images; prostate biopsy; prostate cancer.

## BACKGROUND

Prostate cancer, after lung cancer, is the second largest cause of mortality among males.[1] Prostate-specific antigen (PSA) and digital rectal examination (DRE) play critical roles in diagnosing prostate cancer, and their use has increased the incidence of prostate cancer worldwide. Cancer-related mortality has been reduced as a result of these screening procedures. On the other hand, the PSA and DRE cause overdiagnosis, overtreatment, and unnecessary prostate cancer testing, leading to modifications of prostate cancer recommendations, most notably by the US Preventive Services Task Force (USPSTF) in 2012.[2-4] There has been a significant reduction in PSA testing in the United States since these recommendations were published, along with a decrease in the detection of localized prostate cancer and an increase in the diagnosis of locally progressed and metastatic disease.[5]

We investigated the relationship between prostate tissue resolution and radiation wavelength in the spectrum's infrared area to achieve the stated aim. We also elaborated on the software, allowing us to receive images after infrared radiation to detect prostate cancer confidently.

In 2017, 5 years after the publication of the USPSTF 2012 guideline, there was a rise in prostate cancer "specific mortality" rates and late disease identification in different countries.[6-8] Prostate cancer is now Europe's third biggest cause of mortality in males.[1,9,10]

As a result, imaging modalities of the prostate gland become essential in diagnosing and monitoring prostate cancer.

Our group proposed using infrared rays to visually detect prostate cancer as an alternative and less expensive diagnostic approach than widely-used multiparametric magnetic resonance imaging (mpMRI).[11-15]

We intend to investigate the infrared transmittance of transrectal prostate biopsy tissue to determine the difference between whole prostate tissue and biopsy tissue.

## METHODS

174 formalin-fixed and paraffin-embedded (FFPE) cases (prostate biopsies) were included in the study.

The experimental material was obtained postoperatively (transvesical adenomectomy and radical prostatectomy) from patients with benign prostatic hyperplasia and prostate cancer (Tab.1).

TABLE 1. Distribution of formalin-fixed and paraffin-embedded (FFPE) cases by Gleason score

| Gleason score 6 (3+3) | Gleason score 7 (3+4) | Gleason score 7 (4+3) | Gleason score 8 (4+4) | Gleason score 9 ,10 (4+5), (5+5) |
|---|---|---|---|---|
| 55 | 42 | 31 | 22 | 24 |
| Overall, 174 cases | | | | |

Each FFPE was clamped, and the infrared beam was transmitted through the prostate gland tissue, passed through the lens of the charged-coupled device (CCD) camera, fell on the active matrix of the CCD camera, and transformed into electronic signals (this phenomenon is quite similar to the conversion of light hitting the retina into nerve impulses) transmitted to a computer, where the incoming electrical signals were transformed into visual pictures by special software.

The information from the CCD camera was processed to 256 different levels based on brightness. Ultimately, the "dark" image (corresponding to the state in which prostate tissue absorbs infrared light) was assigned a zero level. Level 255 corresponds to the fact that the prostate does not absorb radiation, and the source infrared light penetrates the CCD chamber. After displaying an infrared image of the prostate on a computer screen, the program identified spots related to cancer and assigned the appropriate code (Fig.1). Healthy areas were also identified under a different code.[16]

FIGURE 1. The formalin-fixed and paraffin-embedded (FFPE) prostate biopsy material visualized by computer software

The program automatically calculated each designated point's corresponding intensity and average value. The process was repeated for visible areas of healthy tissue. The algorithm then computed the ratio of these average intensities. This method was repeated for each subsequent biopsy material and compared with data stored in memory. The computer then computed 90, 95, and 99 percent confidence intervals. When analyzing a new, undiagnosed postsurgical biomaterial, the diagnosis was made by automatically calculating the

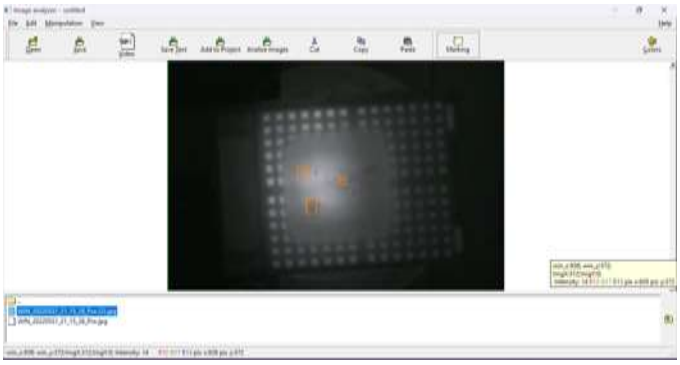

intensity ratio and comparing its compatibility with the recorded standardized data (a fall in the confidence interval of 95% was confirmatory). In addition, computer analysis data were compared with histomorphological results.

All formalin-fixed and paraffin-embedded (FFPE) cases were distributed among five groups by the sum of the Gleason score and the image intensity range (minimal to maximal).

The Statistical Package for Social Sciences (SPSS, version 22) software was used for statistical analysis. Continuous variable differences across groups were compared using a student's t-test. A $p<0.05$ value was considered statistically significant.

## RESULTS

Table 2 represents the characteristics of the different groups.

TABLE 2. Group characteristics by the sum of the Gleason score and the image intensity range

| | Group 1 n=55 | Group 2 n=42 | Group 3 n=31 | Group 4 n=22 | Group 5 n=24 |
|---|---|---|---|---|---|
| **Gleason score** | 6 (3+3) | 7 (3+4) | 7 (4+3) | 8 (4+4), (3+5), 5+3) | 9 (4+5) 10 (5+5) |
| **Intensity (low to high)** | 0.82764 0.88185 | 0.81308 0.87645 | 0.74318 0.87267 | 0.68230 0.71677 | 0.65590 0.70144 |

Figure 2 shows the ranges (minimal to maximal) of image intensities in the different groups of formalin-fixed and paraffin-embedded (FFPE) cases.

FIGURE 2. The ranges of image intensities in different groups

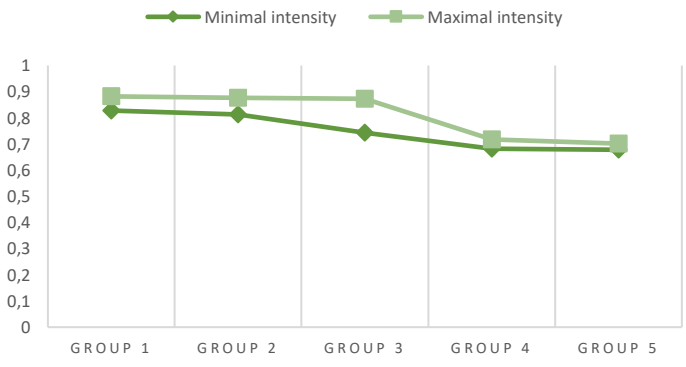


The Georgian Biomedical News
ISSN (Online): 2720-8796 ISSN (Print): 2720-7994

## DISCUSSION

Our results demonstrate a distinct visible difference between prostate cancer tissues with various Gleason scores. Furthermore, the histomorphological evaluation confirmed the changes described above.

In an infrared environment, we investigated prostate cancer biopsy material. The experiment demonstrated that when the Gleason score sum was 6 (3+3) and 7 (3+4) or (4+3), image intensities in the infrared environment were almost indistinguishable from each other, which cannot be said for prostatic gland tissue with a higher Gleason score sum, such as 8 (4+4), (3+ 5) or (5+3), and 9 (4+5) and 10 (5+5). In the latest groups, infrared image intensity was low and close to 0 (dark area).

These differences were not apparent in the first three groups because we used biopsy material with a tissue thickness of 1 mm.

## CONCLUSIONS

Infrared radiation can identify prostate cancer in prostate biopsy tissues. However, further investigations are needed to validate the modality's effectiveness for prostate cancer diagnosis.

## AUTHOR AFFILIATION

1 Department of Urology, Tbilisi State Medical University, Tbilisi, Georgia;
2 Institute of Cybernetics, Georgian Technical University (GTU), Tbilisi, Georgia;
3 Department of Pathology, Tbilisi State Medical University, Tbilisi, Georgia.

## ACKNOWLEDGEMENTS

The SHOTA RUSTAVELI NATIONAL SCIENCE FOUNDATION OF GEORGIA financed this research with the grant "Development of a new method of infrared imaging to prevent cancer recurrence after radical prostatectomy and partial nephrectomy" - code number FR-22-195.

## REFERENCES

1. J. Ferlay, M. Colombet, I. Soerjomataram, et al. Cancer incidence and mortality patterns in Europe: Estimates for 40 countries and 25 major cancers in 2018 Eur J Cancer, 103 (2018), pp. 356-387 Article Download PDF View Record in Scopus Google Scholar
2. D.F. Osses, S. Remmers, F.H. Schröder, T. van der Kwast, M.J. Roobol Results of prostate cancer screening in a unique cohort at 19yr of follow-up Eur Urol, 75 (2019), pp. 374-377 Article Download PDF View Record in Scopus Google Scholar
3. J. Hugosson, M.J. Roobol, M. Månsson, et al. A 16-yr follow-up of the European Randomized Study of Screening for Prostate Cancer Eur Urol, 76 (2019), pp. 43-51 Article Download PDF View Record in Scopus Google Scholar
4. V.A. Moyer, U.S. Preventive Services Task Force Screening for prostate cancer: U.S. Preventive Services Task Force recommendation statement Ann Intern Med, 157 (2012), pp. 120-134 View PDF Cross Ref View Record in Scopus Google Scholar
5. J. Li, Z. Berkowitz, I.J. Hall Decrease in prostate cancer testing following the US Preventive Services Task Force (USPSTF) recommendations J Am Board Fam Med, 28 (2015), pp. 491-493 View PDF Cross Ref View Record in Scopus Google Scholar
6. A. Jemal, M.B. Culp, J. Ma, F. Islami, S.A. Fedewa Prostate cancer incidence 5 years after US Preventive Services Task Force recommendations against screening J Natl Cancer Inst, 113 (2021), pp. 64-71 View PDF Cross Ref Google Scholar
7. S.S. Butler, V. Muralidhar, S.G. Zhao, et al. Prostate cancer incidence across stage, NCCN risk groups, and age before and after USPSTF Grade D recommendations against prostate-specific antigen screening in 2012 Cancer, 126 (2020), pp. 717-724 View PDF Cross Ref View Record in Scopus Google Scholar
8. J.C. Hu, P. Nguyen, J. Mao, et al. Increase in prostate cancer distant metastases at diagnosis in the United States JAMA Oncol, 3 (2017), pp. 705-707 View PDF Cross Ref View Record in Scopus Google Scholar
9. Saskatoon Prostate Cancer Support Group Prostate cancer deaths overtake those from breast cancer. http://spcsg.ca/reading-material/prostate-cancer-deaths-overtake-breast-cancer/ (2019) Google Scholar
10. M. Lenzen-Schulte Prostatakrebs-screening: Prüffall PSA-test Dtsch Arztebl, 117 (2020), pp. 1-2 View Record in Scopus Google Scholar
11. R.L. Siegel, K.D. Miller, A. Jemal Cancer statistics, 2019 CA Cancer J Clin, 69 (2019), pp. 7-34 View PDF Cross Ref View Record in Scopus Google Scholar
12. Partsvania, B., Petriashvili, G., Fonjavidze, N. ,,Possibility of using near infrared irradiation for early cancer diagnosis". Electromagnetic Biology and Medicine, 2014, 33(1), pp. 18–20
13. Khuskivadze A; Partsvania B.; Sulaberidze T. Petriashvili G. 12 th World Cancer Conference. September 26-18 2016, London, UK Journal of Cancer Science and Therapy ISSN: 1948-5956
14. Khuskivadze A.; Kochiashvili G.; Partsvania B.; Chubinidze K.; Sulaberidze T. ,,New Method for enhancement of histo - pathological diagnosis of prostate cancer" Journal of medical and appled sciences. Dol: 10.15520/jmbas. v614-104. 11 april 2018
15. Khuskivadze A.; Partsvania B. Sulaberidze T. Abazadze S. Chubinidze K., An Alternative method for prostate cancer diagnosis" Georgia Europian Urologgy Supplements 18 (12) 2019-3621-3645
16. Sopio Abazadze, Alexandre Khuskivadze, Besarion Partsvania, Tamaz Sulamberidze, Davit Kochiashvili, Omar Khardzeishvili. Infrared Visualization of the Prostate Cancer Georgian Biomedical News. VOLUME 1. ISSUE 1. JANUARY-MARCH 2023.


ISSN (Online): 2720-8796 ISSN (Print): 2720-7994